Stem Cell Reports
Article

ISSCR

OPEN ACCESS

Elevated p53 Activities Restrict Differentiation Potential of MicroRNA-Deficient Pluripotent Stem Cells

Zhong Liu,[1] Cheng Zhang,[3] Maria Skamagki,[2] Alireza Khodadadi-Jamayran,[1] Wei Zhang,[1] Dexin Kong,[1] Chia-Wei Chang,[1] Jingyang Feng,[4] Xiaosi Han,[5] Tim M. Townes,[1] Hu Li,[3] Kitai Kim,[2,*] and Rui Zhao[1,6,*]

[1]Department of Biochemistry and Molecular Genetics, Stem Cell Institute, University of Alabama at Birmingham, Birmingham, AL 35294, USA
[2]Cancer Biology and Genetics Program, Center for Cell Engineering, Center for Stem Cell Biology, Sloan-Kettering Institute, Cell and Developmental Biology Program, Weill Medical College of Cornell University, New York, NY 10065, USA
[3]Department of Molecular Pharmacology and Experimental Therapeutics, Center for Individualized Medicine, Mayo Clinic College of Medicine, Rochester, MN 55905, USA
[4]Cook County Health and Hospital System, John H. Stroger Hospital, Chicago, IL 60612, USA
[5]Department of Neurology, University of Alabama at Birmingham, Birmingham, AL 35294, USA
[6]Gregory Fleming James Cystic Fibrosis Research Center, University of Alabama at Birmingham, Birmingham, AL 35294, USA
*Correspondence: kimk@mskcc.org (K.K.), ruizhao@uab.edu (R.Z.)
https://doi.org/10.1016/j.stemcr.2017.10.006

SUMMARY

Pluripotent stem cells (PSCs) deficient for microRNAs (miRNAs), such as *Dgcr8*$^{-/-}$ or *Dicer*$^{-/-}$ embryonic stem cells (ESCs), contain no mature miRNA and cannot differentiate into somatic cells. How miRNA deficiency causes differentiation defects remains poorly understood. Here, we report that miR-302 is sufficient to enable neural differentiation of differentiation-incompetent *Dgcr8*$^{-/-}$ ESCs. Our data showed that miR-302 directly suppresses the tumor suppressor p53, which is modestly upregulated in *Dgcr8*$^{-/-}$ ESCs and serves as a barrier restricting neural differentiation. We demonstrated that direct inactivation of p53 by SV40 large T antigen, a short hairpin RNA against *Trp53*, or genetic ablation of *Trp53* in *Dgcr8*$^{-/-}$ PSCs enables neural differentiation, while activation of p53 by the MDM2 inhibitor nutlin-3a in wild-type ESCs inhibits neural differentiation. Together, we demonstrate that a major function of miRNAs in neural differentiation is suppression of p53 and that modest activation of p53 blocks neural differentiation of miRNA-deficient PSCs.

INTRODUCTION

MicroRNAs (miRNAs) are small, non-coding RNAs that play important roles in embryogenesis, lineage specification, tissue homeostasis, and human diseases such as neurodegeneration and cancers (Abe and Bonini, 2013; Ivey and Srivastava, 2010; Lee and Dutta, 2009). Biogenesis of miRNAs requires the DROSHA-DGCR8 microprocessor, which cleaves pri-miRNAs into pre-miRNAs, and DICER, which further processes pre-miRNAs into mature miRNAs. Mature miRNAs are then incorporated into the RNA-induced silencing complex (RISC) to destabilize and/or suppress translation of target mRNAs (Ha and Kim, 2014). Notably, *Dgcr8*$^{-/-}$ or *Dicer*$^{-/-}$ embryonic stem cells (ESCs), which have complete miRNA loss, are unable to differentiate into mature somatic cells, indicating that miRNAs are required for differentiation (Kanellopoulou et al., 2005; Liu et al., 2015; Murchison et al., 2005; Wang et al., 2007). Although a number of miRNAs have been identified to facilitate differentiation of wild-type pluripotent stem cells (PSCs) by suppressing pluripotency-promoting genes and/or instructing lineage specification by forming feedforward and feedback regulatory loops with transcriptional regulators (Ivey and Srivastava, 2010; Wang et al., 2007; Xu et al., 2009), no miRNA has yet been reported to rescue the differentiation defects of miRNA-deficient PSCs. Therefore, it remains poorly understood how the lack of miRNAs eliminates the differentiation capacity of PSCs, and which miRNAs are essential to confer differentiation competence.

In this study, we investigated this question by testing the hypothesis that certain miRNAs, most likely those abundantly expressed in PSCs or immediate progenitors, confer differentiation competence to PSCs. We first developed a strategy that allows stable expression of individual miRNAs in miRNA-deficient *Dgcr8*$^{-/-}$ ESCs. Using this strategy, we tested the function of candidate miRNAs in an *in vitro* neural differentiation assay. We chose neural differentiation because our previous data demonstrated that, although incapable of producing any differentiated lineages, embryoid bodies (EBs) formed by *Dgcr8*$^{-/-}$ induced pluripotent stem cells (iPSCs) modestly express markers of neuroectoderm but not mesoderm or endoderm (Liu et al., 2015), which suggested that fewer barriers likely need to be overcome during the differentiation of *Dgcr8*$^{-/-}$ PSCs into neurons. Our data demonstrated that expression of miR-302, which is best known for promoting pluripotency (Melton et al., 2010; Subramanyam et al., 2011; Tiscornia and Izpisua Belmonte, 2010; Wang et al., 2008, 2013), enabled neural differentiation of *Dgcr8*$^{-/-}$ ESCs. We discovered that miR-302 directly suppresses the tumor suppressor p53, which is expressed at a higher basal level in *Dgcr8*$^{-/-}$ ESCs and blocks neural differentiation. Furthermore, direct inactivation of p53 by SV40 large T (LT) antigen, a short

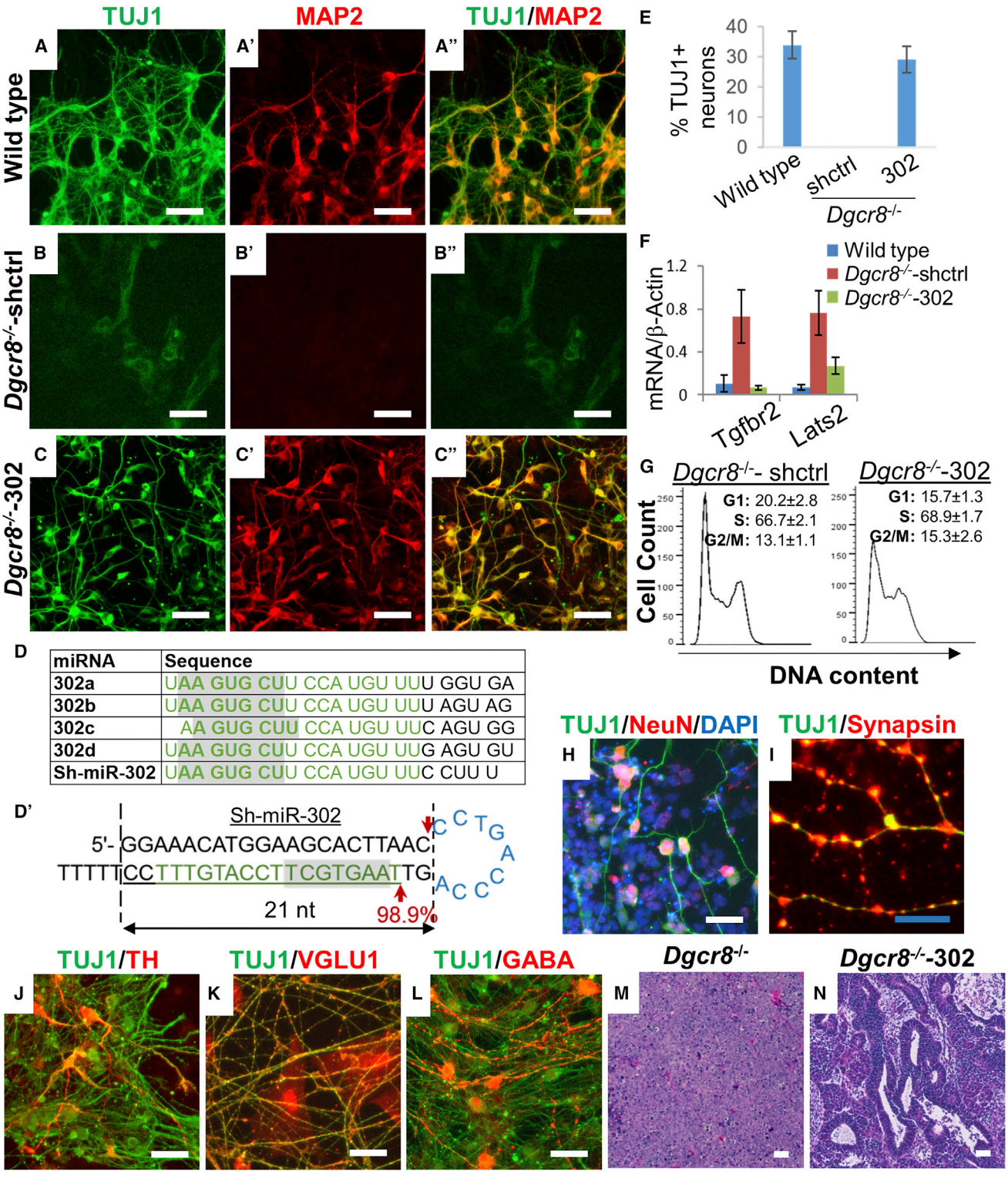

Figure 1. Expression of miR-302 Mimics Enabled Neural Differentiation of *Dgcr8*$^{-/-}$ ESCs

(A–C) Immunostaining of neuron-specific markers TUJ1 (green) and MAP2 (red) in embryoid bodies (EBs) formed by (A–A″) wild-type, (B–B″) *Dgcr8*$^{-/-}$-shctrl, and (C–C″) *Dgcr8*$^{-/-}$-302 ESCs. Scale bars, 50 μm.

(legend continued on next page)

hairpin RNA (shRNA) against *Trp53*, or genetic ablation of *Trp53* enabled neural differentiation of *Dgcr8*$^{-/-}$ PSCs, while activation of p53 in wild-type ESCs by the MDM2 inhibitor nutlin-3a inhibited neural differentiation. Together, our data demonstrate that p53 is a differentiation barrier of miRNA-deficient PSCs and a major function of miRNAs in neural lineage specification is suppression of p53.

RESULTS

Expression of miR-302 Enables Neural Differentiation of *Dgcr8*$^{-/-}$ ESCs

Because *Dicer*$^{-/-}$ or *Dgcr8*$^{-/-}$ PSCs can self-renew but cannot differentiate (Kanellopoulou et al., 2005; Liu et al., 2015; Murchison et al., 2005; Wang et al., 2007), we hypothesized that certain miRNAs, most likely those abundantly expressed in PSCs or immediate progenitors, confer differentiation competence to PSCs. To identify such miRNAs, we expressed mimics of candidate miRNAs into *Dgcr8*$^{-/-}$ ESCs and evaluated the differentiation potential of the resulting cells in an *in vitro* neural differentiation assay (Figures 1A–1C). The top candidate miRNAs included let-7, which induces pluripotency exit (Melton et al., 2010); miR-124 and miR-9, which promote neurogenesis (Kawahara et al., 2012); and miR-302, which is abundantly expressed in PSCs and early neural tissues (Parchem et al., 2014, 2015).

Several studies have identified miRNAs that regulate proliferation, self-renewal, pluripotency exit, and DNA methylation of PSCs by transiently transfecting chemically synthesized miRNA mimics into *Dgcr8*$^{-/-}$ or *Dicer*$^{-/-}$ ESCs (Benetti et al., 2008; Melton et al., 2010; Sinkkonen et al., 2008; Wang et al., 2008). However, because lineage specification often involves multiple rounds of cell division, or takes place over days or even weeks, a strategy that allows stable expression of miRNA mimics would be advantageous. We developed such as method by inserting mature miRNA sequences into lentivirally delivered shRNAs (sh-miRs), which structurally resemble pre-miRNAs and therefore bypass DGCR8 for miRNA biogenesis (Figures 1D and S1). Transcription of shRNAs relies on RNA Pol III-dependent promoters (e.g., the U6 promoter), which preferentially initiate transcription from a guanine (G) residue (Goomer and Kunkel, 1992; Kunkel et al., 1986). However, most RISC-associated mature miRNAs do not have a G residue at the 5′ end (Hu et al., 2009), which makes the 3′ arm of shRNA more suitable than the 5′ arm for miRNA expression. Because the seed sequence, which is between position 2 and 7 on mature miRNAs, is the major determinant for mRNA target selection (Ha and Kim, 2014), the exact sequence and target specificity of a 3′ arm miRNA is determined by the cleaving site of DICER (Figure 1D′). Based on knowledge of how DICER processes stem-loop structures (Gu et al., 2012), we inserted mature miRNA sequences into the 3′ arm starting from the third nucleotide position and kept the stem of the hairpin 21 nucleotides in length (Figure 1D′). Such a design ensures proper processing of the inserted miRNA by DICER.

To validate the neural differentiation assay, we first differentiated wild-type and *Dgcr8*$^{-/-}$ ESCs expressing a control shRNA (*Dgcr8*$^{-/-}$-shctrl). After 14 days of differentiation in EBs, TUJ1+ and MAP2+ neurons were evident in wild-type (Figure 1A–A″) but not *Dgcr8*$^{-/-}$-shctrl ESCs (Figure 1B–B″), confirming that *Dgcr8*$^{-/-}$ PSCs were defective in differentiation (Liu et al., 2015; Wang et al., 2007). Among the tested miRNA mimics (Figures 1 and S2), we discovered that *Dgcr8*$^{-/-}$ ESCs expressing sh-miR-302 (*Dgcr8*$^{-/-}$-302) can efficiently differentiate into TUJ1+ and MAP2+ neurons (Figures 1C–C″ and 1E). RNA sequencing (RNA-seq) analysis demonstrated that 98.9% of miRNAs processed from sh-miR-302 mimicked the endogenous miR-302 (Figure 1D; Table S1), which supports the previous report that small RNAs can be precisely

(D) Expression strategy for sh-miR-302 in *Dgcr8*$^{-/-}$ cells. (D) Sequence alignment of endogenous miR-302 and sh-miR-302. Sequences that are aligned are color labeled (green) and seed sequences are shaded. (D′) Hairpin structure of sh-miR-302. Red arrows represent the predicted Dicer cutting sites. Percentage of correctly processed sh-miRs, which mimics the first 17 nt of the 5′ end of the endogenous miR-302, is presented (see also Table S1).

(E) Percentage (%) of TUJ1+ neuronal cells in total cells (DAPI staining, not shown) of EBs formed in (A–C). Error bars, SD; n = 3 independent biological repeats.

(F) qPCR analyses of known miR-302 targets *Tgfbr2* and *Lats2* (normalized to β-actin) in wild-type, *Dgcr8*$^{-/-}$-shctrl, and *Dgcr8*$^{-/-}$-302 ESCs. Error bar, SD; n = 3 independent biological repeats.

(G) Cell-cycle profile analysis of *Dgcr8*$^{-/-}$-shctrl and *Dgcr8*$^{-/-}$-302 ESCs by DNA content measurement (propidium iodide staining); n = 4, independent biological repeats.

(H–L) Immunostaining of neuron-specific markers TUJ1 (green) and (H) NeuN (red) and DAPI (blue), (I) Synapsin (red), (J) tyrosine hydroxylase (TH) (red), (K) vesicular glutamate transporter 1 (VGLU1) (red), and (L) γ-aminobutyric acid (GABA) (red) in EBs formed by *Dgcr8*$^{-/-}$-302 ESCs. Scale bars, 50 μm (white), 20 μm (blue).

(M and N) H&E staining of teratomas formed by (M) *Dgcr8*$^{-/-}$ ESCs, which contained predominantly undifferentiated cells, and (N) *Dgcr8*$^{-/-}$-302 ESCs, which contained many neuroepithelia. Scale bars, 50 μm. n = 5 independent biological repeats (see also Figure S2).

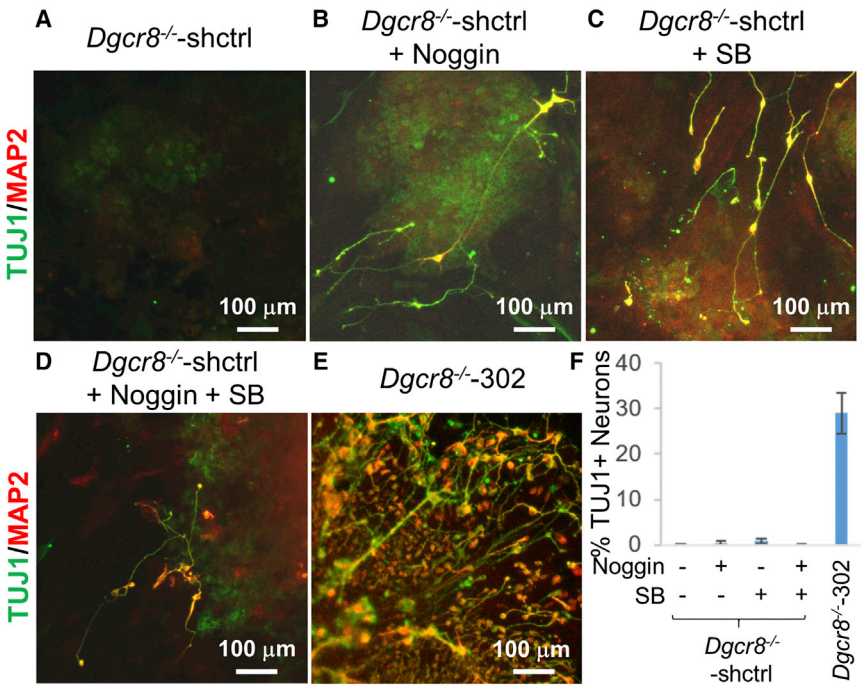

Figure 2. Inhibition of BMP and TGF-β Signaling in *Dgcr8*$^{-/-}$ ESCs Cannot Rescue the Neural Differentiation Defect

(A–E) Immunostaining of neuron-specific markers TUJ1 (green) and MAP2 (red) in EBs formed by (A–D) *Dgcr8*$^{-/-}$-shctrl or (E) *Dgcr8*$^{-/-}$-302 ESCs. During differentiation, EBs of *Dgcr8*$^{-/-}$-shctrl ESCs were treated with (B) Noggin (250 ng/mL), a BMP signaling inhibitor, (C) SB431542 (15 μM), a TGF-β signaling inhibitor, or (D) both.

(F) Percentage (%) of TUJ1+ neuronal cells in total cells (DAPI staining, not shown) of EBs formed in (A–E). Note that inhibition of BMP and/or TGF-β signaling had little effect on induction of neural differentiation, and could not account for the observed sh-miR-302-mediated rescue. Error bars, SD; n = 3 independent biological repeats.

expressed and processed by DICER when inserted into well-designed hairpins (Gu et al., 2012). qPCR analysis confirmed that the known miR-302 mRNA targets *Tgfbr2* and *Lats2*, which were de-repressed in *Dgcr8*$^{-/-}$-shctrl ESCs, were repressed in *Dgcr8*$^{-/-}$-302 ESCs (Figure 1F). Cell-cycle progression from G1 to S phase was significantly accelerated in *Dgcr8*$^{-/-}$-302 ESCs (Figure 1G), consistent with the report that miR-302 accelerate the G1-S phase transition (Wang et al., 2008).

Neurons differentiated from *Dgcr8*$^{-/-}$-302 ESCs expressed the mature neuronal markers NeuN, a post-mitotic neuron-expressed nuclear antigen (Figure 1H), and Synapsin, a membrane protein on synaptic vesicles (Figure 1I). Neurons positive for tyrosine hydroxylase, vesicular glutamate transporter 1, and γ-aminobutyric acid (GABA) (Figures 1J–1L), which are markers for dopaminergic, glutamatergic, and GABAergic neurons, respectively, can also be detected with extended *Dgcr8*$^{-/-}$-302 EB differentiation (28 days). When injected subcutaneously into immunodeficient mice, teratomas formed by *Dgcr8*$^{-/-}$ ESCs contained predominantly undifferentiated cells (Figure 1M), as reported previously (Liu et al., 2015; Wang et al., 2007), whereas teratomas formed by *Dgcr8*$^{-/-}$-302 ESCs consisted of many neuroepithelial tissues (Figure 1N). However, we did not detect obvious mesodermal and endodermal tissues in teratomas formed by *Dgcr8*$^{-/-}$-302 ESCs, suggesting that differentiation into these lineages requires miRNAs other than miR-302.

We attributed the observed rescue of neural differentiation in *Dgcr8*$^{-/-}$ ESCs to functions specific to miR-302. Indeed, expression of let-7, which induces pluripotency exit of *Dgcr8*$^{-/-}$ ESCs (Melton et al., 2010), or of miR-9 and miR-124, two known neurogenesis-promoting miRNAs (Kawahara et al., 2012), failed to rescue the differentiation defect (Figures S2A–S2C). Confirming that the expressed miRNAs were functional, expression of let-7b led to pluripotency exit of *Dgcr8*$^{-/-}$ ESCs as reported by Melton et al. (2010) (Figure S2D–S2D″), while miR-9 and miR-124 downregulated expression of known mRNA target genes (Figures S2E and S2F).

Inhibition of TGF-β and BMP Pathways in *Dgcr8*$^{-/-}$ ESCs Cannot Rescue the Neural Differentiation Defect

Identification of the mRNA targets of miR-302 is critical to understanding how miRNAs regulate the differentiation of PSCs. Among the known miR-302 targets are *Tgfbr2* (Figure 1F), a receptor mediating transforming growth factor-β (TGF-β) signaling, and genes within the bone morphogenetic protein (BMP) signaling pathway (Lipchina et al., 2011; Subramanyam et al., 2011). Because inhibition of TGF-β and BMP pathways induces efficient neural differentiation (Chambers et al., 2009), we tested whether sh-miR-302 enabled neural differentiation of *Dgcr8*$^{-/-}$ ESCs by repressing these pathways. We demonstrated that inhibition of the TGF-β pathway with the chemical inhibitor SB431542 and/or inhibition of the BMP pathway by Noggin in *Dgcr8*$^{-/-}$ ESCs had little effect on neural

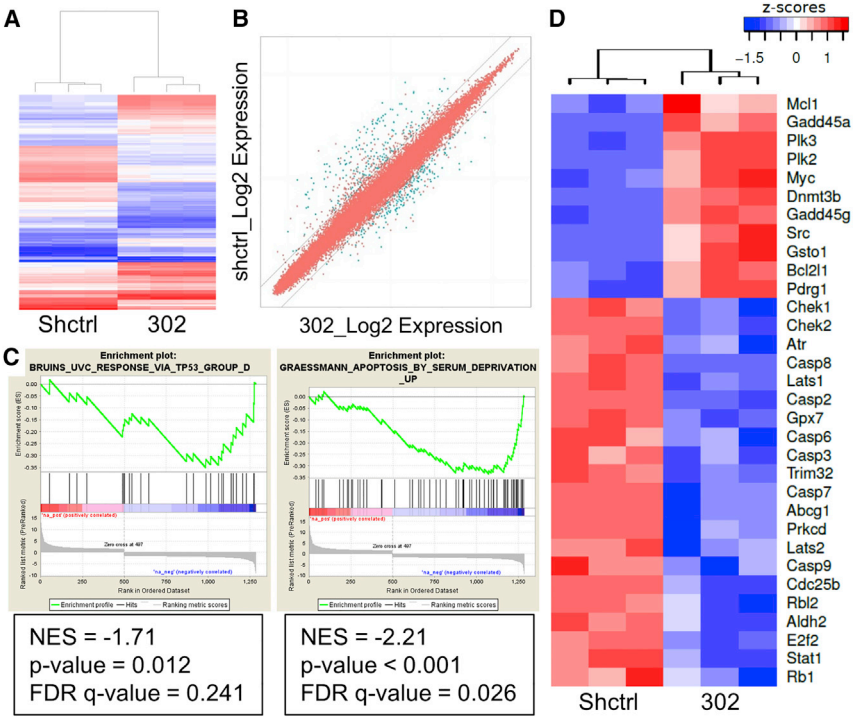

Figure 3. Expression Profiling Reveals that sh-miR-302 Suppresses p53 Target Genes in *Dgcr8*$^{-/-}$ ESCs

(A) Unsupervised clustering analysis segregates biological repeats of *Dgcr8*$^{-/-}$-shctrl ESCs (n = 3) from *Dgcr8*$^{-/-}$-302 ESCs (n = 3 independent biological repeats).

(B) Scatterplot showing that ectopic expression of miR-302 leads to upregulation of 643 genes and downregulation of 942 genes by 1.5-fold ($p < 0.05$) in *Dgcr8*$^{-/-}$ ESCs. Green dots represent the significantly differentially expressed genes between the *Dgcr8*$^{-/-}$-shctrl and *Dgcr8*$^{-/-}$-302 ESCs groups (see also Table S2).

(C) Gene set enrichment analysis (GSEA) reveals that genes regulated by p53 or upregulated in apoptosis are repressed in *Dgcr8*$^{-/-}$ ESCs by sh-miR-302 (see also Table S3).

(D) Heatmap showing differential expression of selected genes between *Dgcr8*$^{-/-}$-shctrl and *Dgcr8*$^{-/-}$-302 ESCs.

differentiation (Figures 2A–2D), and therefore could not fully account for the effect of sh-miR-302 expression (Figures 2E and 2F).

p53 Is a Differentiation Barrier in PSCs

To gain insight into how miR-302 enables neural differentiation of *Dgcr8*$^{-/-}$ ESCs, we compared expression profiles of *Dgcr8*$^{-/-}$-shctrl and *Dgcr8*$^{-/-}$-302 ESCs by microarray analysis. Expression of sh-miR-302 resulted in upregulation of 643 genes and downregulation 941 genes by 1.5-fold ($p < 0.05$) in *Dgcr8*$^{-/-}$ ESCs (Figures 3A and 3B; Table S2). Gene set enrichment analysis (GSEA) revealed downregulation of multiple gene sets in *Dgcr8*$^{-/-}$-302 ESCs (Table S3), including genes regulated by p53 or induced by conditions related to p53 activation, such as apoptosis (Figures 3C and 3D). These data led us to hypothesize that increased p53 activity, which is normally suppressed by miR-302, blocks neural differentiation in *Dgcr8*$^{-/-}$ ESCs.

To test this hypothesis, we ectopically expressed the SV40 LT antigen, which inactivates both p53 and all RB family proteins (An et al., 2012) in *Dgcr8*$^{-/-}$ ESCs (*Dgcr8*$^{-/-}$-LT). TUJ1+, MAP2+, and NeuN + neurons were readily detected in EBs formed by *Dgcr8*$^{-/-}$-LT ESCs (Figures 4A and 4B). To separate the roles of p53 and the RB family proteins, we ectopically expressed an shRNA against p53 (*Dgcr8*$^{-/-}$-shp53) or T121 (*Dgcr8*$^{-/-}$-T121), a truncated version of the LT antigen that only inactivates RB proteins (Ewen et al., 1989), in *Dgcr8*$^{-/-}$ ESCs. Neurons expressing TUJ1, MAP2, and NeuN were evident in EBs formed by *Dgcr8*$^{-/-}$-shp53 ESCs (Figures 4C and 4D), but were rarely seen in EBs formed by *Dgcr8*$^{-/-}$-T121 ESCs (Figure 4E). qPCR analysis verified a reduction of *Trp53* mRNA in *Dgcr8*$^{-/-}$-shp53 ESCs to 25%–30% of that in *Dgcr8*$^{-/-}$-shctrl ESCs (Figure 4F), suggesting that an increase in p53 by 3- to 4-fold could block differentiation of *Dgcr8*$^{-/-}$ ESCs. In addition, teratomas of *Dgcr8*$^{-/-}$-shp53 ESCs contained primarily neural tissues but not mesodermal and endodermal derivatives (Figure 4G).

We also generated iPSCs deficient for both *Dgcr8* and *Trp53* (*Dgcr8*$^{-/-}$;*Trp53*$^{-/-}$ iPSCs) from tail tip fibroblasts of *Dgcr8*$^{flox/flox}$;*Trp53*$^{flox/flox}$ mice. Consistently, *Dgcr8*$^{-/-}$;*Trp53*$^{-/-}$ iPSCs efficiently differentiated into TUJ1+, MAP2+, and NeuN + neurons (Figures 4H and 4I), in contrast to *Dgcr8*$^{-/-}$ iPSCs, which were differentiation incompetent (Liu et al., 2015). Furthermore, wild-type ESCs treated with nutlin-3a (Figure 4J), a small molecule that stabilizes p53 (Vassilev et al., 2004), exhibited greatly reduced neural differentiation (Figures 4K and 4L). Together, these data demonstrate that elevated p53 activities block neural differentiation of PSCs.

p53 Is Directly Suppressed by miR-302

To explore the mechanism by which p53 is regulated by miR-302, we conducted a computational search and identified a putative miR-302 recognition site on the 3′ UTR of p53 (Figure 5A). Although mRNA of *Trp53* is expressed at similar levels (Figure 5B), we found that *Dgcr8*$^{-/-}$ ESCs

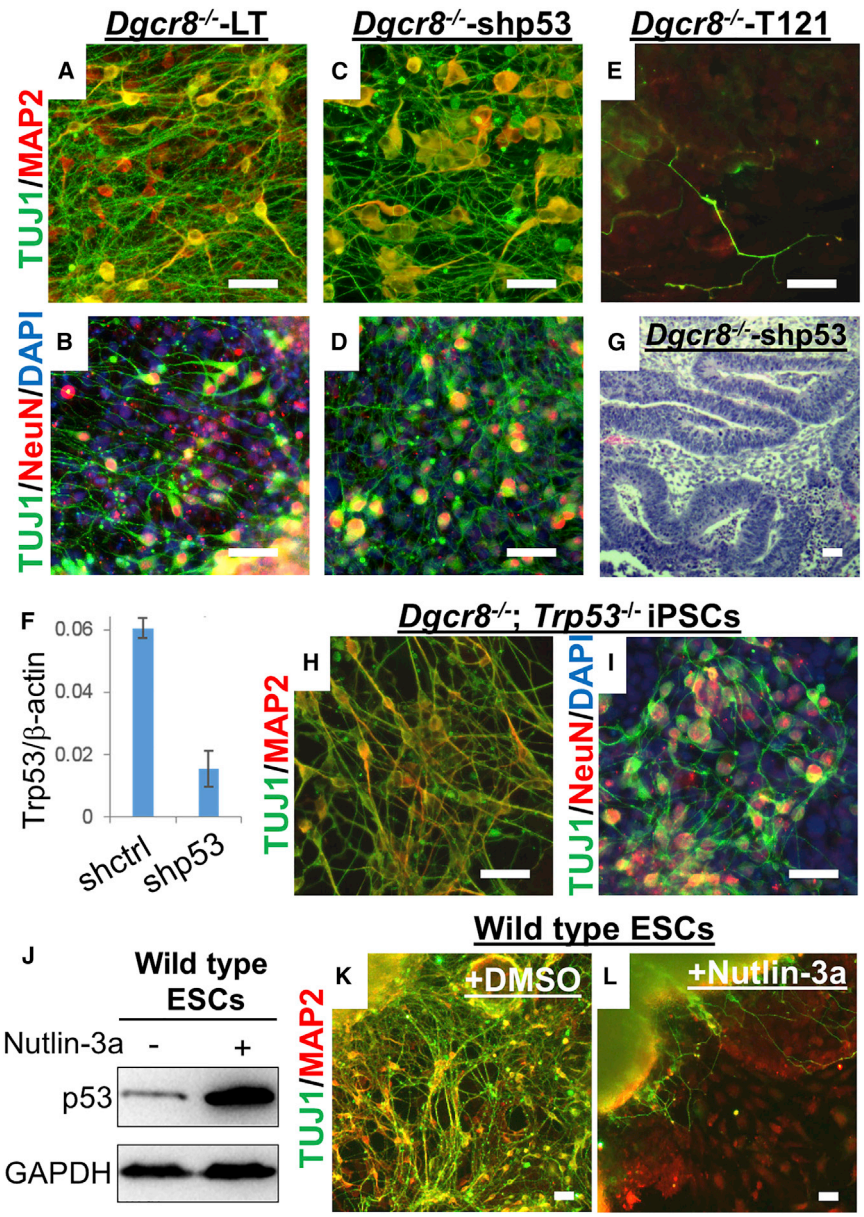

Figure 4. Elevated p53 Activity Serves as a Barrier Blocking Differentiation of *Dgcr8*$^{-/-}$ and Wild-Type PSCs

(A–E) Immunostaining of neuron-specific markers TUJ1 (green), MAP2 (red in A, C, and E), and NeuN (red in B and D) in EBs formed by *Dgcr8*$^{-/-}$ ESCs expressing (A and B) the SV40 large T antigen (*Dgcr8*$^{-/-}$-LT), (C and D) an shRNA against p53 (*Dgcr8*$^{-/-}$-shp53), or (E) T121 (*Dgcr8*$^{-/-}$-T121), a truncated large T antigen that only inactivates RB family proteins. Scale bars, 50 μm.

(F) qPCR analysis of p53 in *Dgcr8*$^{-/-}$-shctrl and *Dgcr8*$^{-/-}$-shp53 ESCs confirms p53 knockdown. Error bars, SD; n = 3 independent biological repeats.

(G) H&E staining of teratomas formed by *Dgcr8*$^{-/-}$-shp53 ESCs, which contain many neuroepithelia. Scale bars, 50 μm. n = 3 independent biological repeats.

(H and I) Immunostaining of neuron-specific markers TUJ1 (green) and (H) MAP2 (red) and (I) NeuN (red) in EBs formed by *Dgcr8*$^{-/-}$; *Trp53*$^{-/-}$ iPSCs. Scale bars, 50 μm.

(J) Immunoblotting of p53 and GAPDH in wild-type ESCs treated with DMSO or nutlin-3a.

(K and L) Immunostaining of TUJ1 (green) and MAP2 (red) in EBs formed by wild-type ESCs treated with (K) DMSO or (L) nutlin-3a. Scale bars, 50 μm.

express approximately 3- to 4-fold higher levels of p53 protein than the wild-type or *Dgcr8*$^{-/-}$-302 ESCs (Figure 5C). To test the functionality of the miR-302 recognition site, we performed a luciferase reporter assay. We generated luciferase reporters containing the intact 3′ UTR of p53 (WT-Luc) or a mutant 3′ UTR (Mut-Luc), which contains two mutated nucleotides within the seed sequence of the miR-302 recognition site (Figure 5D). We also generated a positive control reporter (302-Luc) by inserting a sequence fully complementary to miR-302d. miR-302 effectively suppressed luciferase activities of the 302-Luc and WT-Luc reporters, but not the Mut-Luc reporter (Figure 5E), which indicates that the miR-302 recognition site is functional and p53 is directly suppressed by miR-302.

p53 Is Upregulated in *Dgcr8*$^{-/-}$ ESCs

Because p53 activation often leads to apoptosis, and PSCs are known to be sensitive to genotoxic insult (Aladjem et al., 1998; Hong and Stambrook, 2004; Roos et al., 2007), it was puzzling that *Dgcr8*$^{-/-}$ ESCs could tolerate elevated p53 activity. We found that p53 can be further induced in *Dgcr8*$^{-/-}$ ESCs by the DNA-damaging reagent neocarzinostatin (NCS) (Figure 6A). While wild-type ESCs did not undergo an obvious cell-cycle arrest upon NCS treatment, which agrees with previous reports (Aladjem

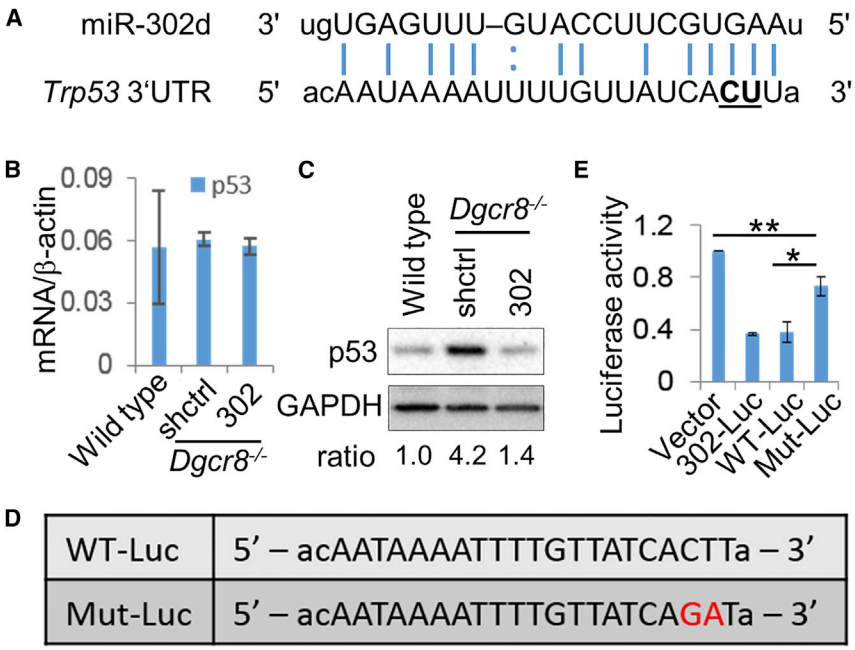

Figure 5. miR-302 Directly Suppresses p53 Expression

(A) Computational analysis predicting a miR-302 recognition site on the 3′ UTR of p53. The nucleotides mutated in the Mut-Luc reporter are underlined.

(B) qPCR analysis demonstrating that *Trp53* is expressed at similar levels in wild-type, *Dgcr8*$^{-/-}$-shctrl, and *Dgcr8*$^{-/-}$-302 ESCs. Error bars, SD; n = 3–6 independent biological repeats.

(C) Immunoblotting of p53 and GAPDH in wild-type, *Dgcr8*$^{-/-}$, and *Dgcr8*$^{-/-}$-302 ESCs. Quantification of p53 was determined by ImageJ (normalized to GAPDH). n = 3 independent biological repeats.

(D) Sequences of the miR-302 recognition site on luciferase reporters. WT-Luc and Mut-Luc, the intact and mutant 3′ UTR of p53, respectively. The mutated nucleotides are shown in red.

(E) Luciferase reporter assay. Vector, empty pSicheck2 luciferase vector; 302-Luc, positive control reporter with sequence fully complementary to miR-302d. n = 3 independent biological repeats; *p < 0.05; **p < 0.01; Student's t test.

et al., 1998; Qin et al., 2007), NCS-treated *Dgcr8*$^{-/-}$ ESCs exhibited clear cell-cycle arrest, as demonstrated by the marked reduction of bromodeoxyuridine (BrdU)-labeled S phase cells and accumulation of G2/M phase cells (Figures 6B and 6C). Interestingly, NCS treatment had little effect on the cell cycle of *Dgcr8*$^{-/-}$-302 ESCs, which is similar to what was seen in wild-type ESCs (Figures 6B and 6C). Compared with wild-type and *Dgcr8*$^{-/-}$-302 ESCs, induction of p53 by NCS is more efficient in *Dgcr8*$^{-/-}$ ESCs (Figure 6A), likely due to the lack of miR-302-mediated p53 suppression. Because the biological outcomes of p53 activation may be determined by the magnitude of activated p53 (Purvis et al., 2012), it is likely that the higher p53 levels in *Dgcr8*$^{-/-}$ ESCs contribute to the differences in cell-cycle regulation.

Next, we investigated how p53 level regulates the dual roles of p53 in ESCs: differentiation suppression and apoptosis induction. We first induced p53 expression in wild-type ESCs in a nutlin-3a dose-dependent manner (Figure 7A), and examined apoptosis of the nutlin-3a-treated ESCs. We found that increased levels of p53 had little effect on apoptosis rates of the nutlin-3a-treated ESCs, as determined by Annexin V staining (Figures 7B and 7C). This was surprising because ESCs are known to be sensitive to genotoxic insults (Aladjem et al., 1998; Hong and Stambrook, 2004; Roos et al., 2007). We then examined how ESCs respond to the DNA-damaging chemical NCS. We found that NCS strongly induced apoptosis in ESCs (Figures 7B and 7C), although NCS-induced p53 expression did not reach the levels induced by high doses of nutlin-3a (Figure 7A). These data demonstrated that apoptosis does not correlate well with p53 level in ESCs. In agreement with our data, Aladjem et al. (1998) reported that p53-null ESCs undergo apoptosis at a similar rate as wild-type ESCs in response to DNA damage, demonstrating that DNA damage-induced apoptosis may be executed via a p53-independent mechanism in ESCs. Because nutlin-3a is known to induce p53 by blocking MDM2-mediated p53 degradation without inducing DNA damage (Vassilev et al., 2004), our data suggested that increased p53 expression without DNA damage does not efficiently induce apoptosis in ESCs (Figures 7A–7C); however, such an increase strongly inhibited differentiation (Figures 4J–4L). Taken together, our data demonstrated that activation of p53, which is normally suppressed by miRNAs such as miR-302, serves as a barrier that restricts neural differentiation of PSCs (Figure 7D).

DISCUSSION

The miR-302 family, which is most abundantly expressed in epiblast-derived pluripotent stem cells and human ESCs (Card et al., 2008; Parchem et al., 2014; Suh et al.,

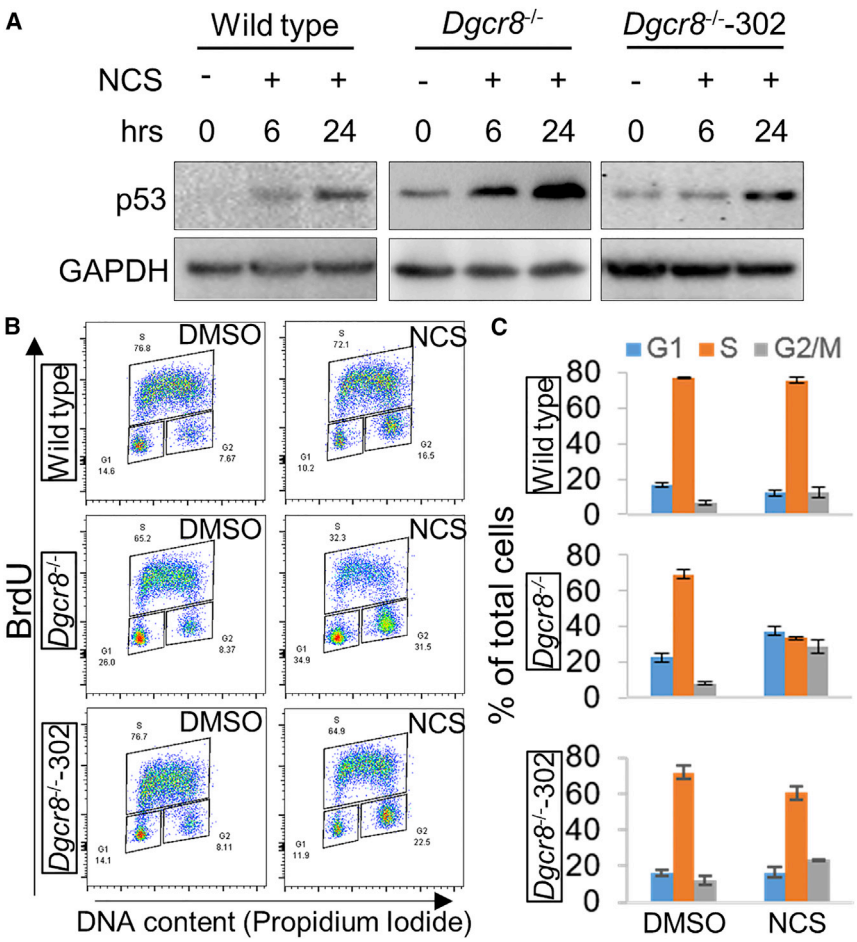

Figure 6. p53 Is Moderately Activated in *Dgcr8*$^{-/-}$ ESCs

(A) Immunoblotting of p53 in wild-type, *Dgcr8*$^{-/-}$, and *Dgcr8*$^{-/-}$-302 ESCs treated with neocarzinostatin (NCS) for the indicated times. Immunoblotting of GAPDH served as a loading control.

(B) NCS treatment causes cell-cycle arrest in *Dgcr8*$^{-/-}$ ESCs. Shown are representative fluorescence-activated cell sorting (FACS) plots of BrdU pulse-labeled ESCs 24 hr after DMSO (control) or NCS treatment in wild-type, *Dgcr8*$^{-/-}$, and *Dgcr8*$^{-/-}$-302 ESCs.

(C) Quantification of NCS-induced cell-cycle arrest. Error bars, SD; n = 4 independent biological repeats.

2004), is generally believed to promote pluripotency by facilitating rapid cell-cycle progression and antagonizing the differentiation-inducing activities of let-7 miRNAs (Melton et al., 2010; Wang et al., 2008). Furthermore, miR-302 enhances iPSC derivation when co-expressed with the Yamanaka factors (Leonardo et al., 2012). In this study, we demonstrated that miR-302 promotes lineage specification by inhibiting p53 activation. Interestingly, inhibition of p53 has also been shown to enhance iPSC derivation (Spike and Wahl, 2011). Our data suggest that, among the many mechanisms that promote reprogramming, miR-302 may also facilitate reprogramming by suppressing p53 expression. Several other pluripotency transcriptional regulators, including OCT4, SOX2, and NANOG, have also been demonstrated to promote lineage specification (Frum et al., 2013; Graham et al., 2003; Messerschmidt and Kemler, 2010). These data therefore suggest that it is a general attribute of pluripotency regulators to play dual roles (i.e., promoting self-renewal and inducing lineage specification) in different cellular contexts.

Dicer$^{-/-}$ or *Dgcr8*$^{-/-}$ mice embryos die before formation of body axis, underscoring an essential role of miRNAs in early embryogenesis (Bernstein et al., 2003; Wang et al., 2007). Tissue-specific disruption of *Dicer* or *Dgcr8* has been performed to evaluate the roles of miRNAs in a variety of tissues, such as cerebral cortex and neuron types (Choi et al., 2008; Davis et al., 2008; De Pietri Tonelli et al., 2008; Kawase-Koga et al., 2009; Kim et al., 2007; Makeyev et al., 2007), neural crest (Chapnik et al., 2012; Nie et al., 2011), hair follicles (Andl et al., 2006), limb mesoderm (Harfe et al., 2005), and immune cells (Cobb et al., 2005). Interestingly, phenotypes associated with p53 activation, such as reduced proliferation and/or increased apoptosis, have been observed in virtually all such studies. Whether p53 activation contributes to the observed phenotypic defects in all these tissues remains an open question. Furthermore, we observed that teratomas formed by *Dgcr8*$^{-/-}$-302 or *Dgcr8*$^{-/-}$-shp53 ESCs contained primarily neural tissues but no obvious mesodermal and endodermal lineages. These data suggest that a major role of miRNAs in PSC differentiation into the neural lineage is to suppress p53 activation, while additional p53-independent functions of miRNAs are likely necessary for the differentiation of mesodermal and endodermal tissues.

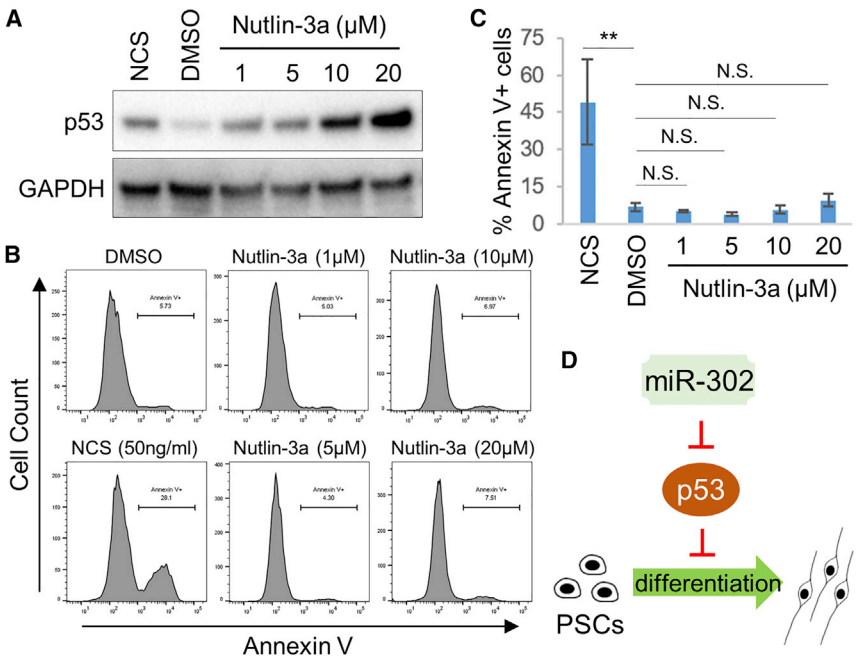

Figure 7. Increased p53 Expression without DNA Damage Does Not Efficiently Induce Apoptosis in ESCs

(A) Immunoblotting of p53 in ESCs treated with NCS or increasing concentrations of nutlin-3a. GAPDH was used as a loading control.

(B) Apoptosis of wild-type ESCs treated with NCS or nutlin-3a. Shown are representative FACS plots of Annexin V staining. DMSO-treated ESCs were used as a negative control.

(C) Quantification of apoptosis of wild-type ESCs treated with NCS or nutlin-3a. Error bars, SD; n = 3–7 independent biological repeats. **p < 0.01; N.S., not significant; two-tailed Student's t test.

(D) A model illustrating that miR-302 directly suppresses p53 expression and elevated p53 blocks neural differentiation.

Several lines of evidence suggest that, on the molecular level, p53 activation suppresses self-renewal and induces exit from pluripotency. p53 directly inhibits *Nanog* expression, suggesting a mechanism to eliminate damaged cells from the stem cell pool by inducing differentiation (Lin et al., 2005). Furthermore, p53 activated by DNA damage was demonstrated to bind promoters and enhancers of hundreds of genes, with a tendency of repressing genes for self-renewal and activating genes for differentiation (Li et al., 2012). However, whether these p53-induced transcriptional changes are sufficient to promote differentiation of PSCs has not been demonstrated. In this study, we found that miRNA deficiency moderately activates p53, which is sufficient to block differentiation of PSCs. Because the biological outcomes of p53 activation may be determined by the types of stress signals and the magnitude and duration of activated p53 (Horn and Vousden, 2007; Kastenhuber and Lowe, 2017; Khoo et al., 2014; Purvis et al., 2012), it is also likely that the moderately upregulated basal expression of p53 in *Dgcr8*$^{-/-}$ ESCs may lead to biological outcomes different from those elicited by full p53 activation upon genotoxic insult.

Activation of p53 regulates many biological processes, such as cell-cycle progression, cell viability, senescence, and metabolism (Kruse and Gu, 2009). All of these pathways have been shown to contribute to the tumor suppressor function of p53. Many of these known functions of p53 may also contribute to differentiation suppression. After NCS treatment, we observed that *Dgcr8*$^{-/-}$ ESCs are more prone to cell-cycle arrest compared with wild-type and *Dgcr8*$^{-/-}$-302 ESCs (Figures 6B and 6C). Therefore, it is possible that increased cell-cycle arrest during differentiation could suppress tissue differentiation. Furthermore, it is possible that additional p53-mediated functions (e.g., apoptosis, senescence, etc.) are also differentially regulated, which might together contribute to the differentiation incompetence of *Dgcr8*$^{-/-}$ ESCs.

p53, referred to as the cellular gatekeeper or the guardian of the genome, is best known for its roles in responding to cellular stress and protection of genome integrity (Lane, 1992; Levine, 1997). Because *Trp53*$^{-/-}$ mouse embryos can develop into adulthood but succumb to tumors by 6 months of age (Donehower et al., 1992), p53 was thought to play a minimal role in embryo development. However, because most tumors arise in individuals later in life, it has been postulated that p53 must be evolutionarily selected by other non-tumor suppressor functions that are critical to earlier stages of life (Hu et al., 2008; Lu et al., 2009). Our data suggest that activation of p53 by a major genetic defect, such as miRNA deficiency, could serve as a potential mechanism to eliminate genetically defective embryos at very early stage of pregnancy to save maternal resources.

EXPERIMENTAL PROCEDURES

Cell Culture and EB Differentiation

Mouse ESCs and iPSCs were passaged in mouse ESC maintenance medium (DMEM, 15% fetal bovine serum [FBS; Gemini Bio], 0.1 mM non-essential amino acid [NEAA, Thermo Fisher Scientific],

0.1 mM β-mercaptoethanol [β-ME, Sigma-Aldrich], and 1,000 U/mL mouse LIF [ESGRO, EMD Millipore]) on gelatin-coated tissue culture plates as described previously (Liu et al., 2015). For EB differentiation, trypsinized ESCs were suspended in Costar ultra-low-attachment cell culture plates (Corning) at a density of 1×10^5 cells/ml in EB medium (DMEM, 15% Knockout Serum Replacement [Thermo Fisher Scientific], 0.1 mM NEAA, 0.1 mM β-ME) for 4 days. The EBs were seeded onto gelatin-coated plates at a density of 5 EB/cm^2 and continued in culture in EB medium for 14 days. For nutlin-3a treatment, ESCs were differentiated in EB medium with 10 μM nutlin-3a (Cayman Chemicals). For inhibition of TGF-β and/or BMP signaling, ESCs were differentiated in EB medium containing 15 μM SB431542 (Sigma-Aldrich) and/or 250 ng/mL Noggin (PeproTech). EB medium was changed every other day.

Vector Construction and Lentiviral Production

Sh-miRs and shRNAs were cloned into the lentiviral vector pLKO.1 at AgeI and EcoRI sites, as described previously (Moffat et al., 2006). DNA fragments containing the lLT antigen and T121 were PCR amplified from the pBABE-puro-SV40 LT plasmid (Addgene, no. 14088) (Zhao et al., 2003) and recombined into the pSINE-EF2-DEST-Pur lentiviral vector (Liu et al., 2015) using Gateway Technology (Thermo Fisher Scientific). Lentivirus was prepared as described previously (Zhao et al., 2014). Oligonucleotides used are listed in Table S4.

Immunostaining

Immunostaining was performed as described previously (Liu et al., 2017). In brief, EBs were fixed in 4% paraformaldehyde, blocked in Protein Block (Dako), and incubated with the appropriate primary antibodies overnight at 4°C and secondary antibodies for 1 hr at room temperature. Nuclei were counterstained by 0.5 μg/mL DAPI. Images were acquired by a Nikon Ti-S microscope and processed by Photoshop CS6. Antibodies used were TUJ1 (801202, BioLegend), MAP2 (sc-20172, Santa Cruz), NeuN (MAB377, Millipore), Synapsin (AB1543, Millipore), tyrosine hydroxylase (P40101, Pel-Freez), VGLU1 (135302, Synaptic Systems), and GABA (A2052, Sigma-Aldrich).

Mice, Teratoma Analysis, and iPSC Derivation

All animal experiments were performed in accordance with guidelines from the University of Alabama at Birmingham (UAB) and NIH. Teratoma injection was performed as described previously (Liu and Zhao, 2016). Non-obese diabetic severe combined immunodeficiency gamma mice (Jackson Laboratory) 4–10 weeks of age were injected subcutaneously with 1×10^6 to 5×10^6 ESCs. Tumors were harvested, fixed with 10% formalin, and processed by the UAB Comparative Pathology Laboratory. Tail tip fibroblasts (TTFs) were isolated from 2-week-old *Dgcr8*$^{flox/flox}$;*Trp53*$^{flox/flox}$ mice (Marino et al., 2000; Wang et al., 2007) and cultured in D10 medium (DMEM, 10% FBS). Derivation of iPSCs was performed as described previously (Liu et al., 2015), which involves transduction of TTFs with STEMCCA lentivirus at MOI of 2, plating cells onto irradiated MEF feeders, and culturing in ESC maintenance medium for 3 weeks. Inactivation of *Dgcr8* and *Trp53* were achieved by transduction of a Cre-expressing retrovirus (Addgene, no. 24064).

Cell-Cycle and Apoptosis Analysis

BrdU pulse labeling and cell-cycle analysis were performed as described previously (Zhao et al., 2014). In brief, cells at 50% confluency were pulse-labeled with 10 μM BrdU (Sigma-Aldrich) 30 min before trypsinization and fixation in cold 70% ethanol at −20°C overnight. Cells were washed twice in PBS, denatured in 2N HCl containing 1% Triton X-100 at room temperature for 30 min, neutralized by 0.1 M sodium borate (pH 8.5), washed and resuspended in PBS containing 1% BSA and 0.5% Tween 20, and stained by APC-conjugated BrdU antibody (BioLegend) and 5 μg/mL propidium iodide. Cells were analyzed on a BD Fortessa flow cytometer. Apoptosis analysis was performed as described previously (Liu et al., 2017). In brief, ESCs were treated with the indicated concentration of nutlin-3a or 50 ng/mL NCS (Sigma-Aldrich) for 24 hr. Cells were trypsinized, stained with APC-conjugated Annexin V (BD Biosciences) on ice for 15 min and 1 μg/mL of propidium iodide (Sigma-Aldrich) at room temperature for 5 min, and then analyzed on a BD Fortessa flow cytometer. Data were analyzed by the FlowJo VX software.

RNA Extraction and qPCR

Total RNA was isolated with the DirectZol RNA Kit (Zymo Research) and cDNA were synthesized by the Verso cDNA Synthesis Kit (Thermo Fisher Scientific). qPCR was performed using 2× Absolute Blue Q-PCR Master Mix (Thermo Fisher Scientific) on a ViiA 7 real-time PCR system (Thermo Fisher Scientific). Primers are listed in Table S4.

Immunoblotting

Immunoblotting was performed as described previously (Liu et al., 2015). Whole-cell extracts were prepared in RIPA buffer (50 mM Tris-HCl [pH 8.0], 150 mM NaCl, 1% NP-40, 0.5% sodium deoxycholate, and 0.1% SDS), separated on a 4%–20% SDS-polyacrylamide gel (Bio-Rad), and transferred to polyvinylidene fluoride membrane (Thermo Fisher Scientific). For NCS treatment, 50 ng/mL NCS (Sigma-Aldrich) was added into medium and extracts were collected at the indicated times. Antibodies used were p53 (sc-6243) and glyceraldehyde-3-phosphate dehydrogenase (sc-25778, Santa Cruz).

Luciferase Assay

The full-length wild-type 3′ UTR of p53 was chemically synthesized and cloned into the pUC57 vector (Genewiz). The wild-type 3′ UTR of p53 was then subcloned into the pSiCheck2 plasmid (Promega) at XhoI and NotI sites to generate the WT-Luc reporter. Mutations at the miR-302 recognition site were introduced by PCR-based site-directed mutagenesis, as described previously (Zhao et al., 2014) to generate the Mut-Luc reporter. To generate the 302-Luc reporter, oligonucleotides complementary to miR-302d were ligated into the pSiCheck2 plasmid at XhoI and NotI sites. Oligonucleotides used for luciferase reporter construction are listed in Table S4. All constructs were confirmed by Sanger sequencing. Forty-eight hours before the luciferase assay, 3×10^3 HEK293T cells were transfected with 5 ng of luciferase reporters and 3 pmol of miR-302d mimic or control mimic conjugated with Dy547 (C-310372-05 and CP-004500-01, GE Dharmacon) by Lipofectamine 2000 (Thermo Fisher Scientific).

Luciferase activity was measured using the Dual-Luciferase Reporter Assay System as per the manufacturer's instructions (Promega) on a Synergy H1 Hybrid Multi-Mode Microplate Reader (BioTek).

Microarray, Small RNA-Seq, and Data Analysis

Global expression profiles were determined using the GeneChip Mouse Gene 2.0 ST Array (Affymetrix) at the Coriell Genotyping and Microarray Center. Raw microarray signal intensities were robust multiarray average summarized and quantile normalized using R/BioConductor (Bolstad et al., 2003; Gentleman et al., 2004; Irizarry et al., 2003). To detect differentially expressed genes, Student's t tests were performed on pairwise comparisons between *Dgcr8*$^{-/-}$-shctrl and *Dgcr8*$^{-/-}$-302 ESCs groups. We applied q value to t test p values to estimate the false discovery rate (Storey and Tibshirani, 2003), and set fold change larger than 1.5, and $p < 0.05$ as the threshold for determining the number of differentially expressed genes between groups. We used hierarchical clustering on the z score-transformed expression values of selected genes with the "complete" linkage method based on Euclidean distance to order the genes in the heatmap. Heatmap and scatterplot visualizations were performed in R (v.3.0.2) using the gplots and ggplot2 packages. GSEA analysis was performed according to Subramanian et al. (2005). Small RNA-seq was used to confirm sh-miR-302 expression. Total RNA was extracted from *Dgcr8*$^{-/-}$-302 cells and submitted to the Genomic Services Lab at the HudsonAlpha Institute. The library was constructed by the standard miRNA library construction protocol (Illumina) and 15 million, 50 bp single-end reads were acquired. Adapters were removed from the reads using cutadapt (v.1.8.1) (Anders et al., 2015). All the reads were mapped to the mouse reference genome (GRCm38.74/mm10) using STAR aligner guided by a Gene Transfer File (Ensembl GTF version GRCm38.74) (Dobin et al., 2013).

ACCESSION NUMBERS

The accession number for the expression data is GEO: GSE104569.

SUPPLEMENTAL INFORMATION

Supplemental Information includes Supplemental Experimental Procedures, two figures, and four tables and can be found with this article online at https://doi.org/10.1016/j.stemcr.2017.10.006.

AUTHOR CONTRIBUTIONS

Z.L., K.K., and R.Z. conceived the experimental plan. Z.L., M.S., W.Z., D.K., C.-W.C., and J.F. performed experiments. C.Z., A.K.-J., and H.L. performed computational analysis. Z.L., X.H., T.M.T., H.L., K.K., and R.Z wrote the manuscript.

ACKNOWLEDGMENTS

R.Z. is supported by the UAB startup fund, UAB Faculty Development Fund, and UAB CFRC Pilot & Feasibility Grant (ROWE15R0). K.K. is supported by the NIH (R00HL093212 and R01AG043531), the TriStem-Star Foundation (2013-049), Louis V. Gerstner, Jr. Young Investigators awards, the Geoffrey Beene Junior Chair Award, the Sidney Kimmel Scholar Award, the Alfred W. Bressler Scholars Endowment Fund, and the MSKCC Society Fund. H.L. is supported by the NIH (CA196631-01A1), the Paul F. Glenn Foundation, and the Mayo Clinic Center for Individualized Medicine. X.H. is supported by the NIH (R01NS095626).

Received: June 1, 2017
Revised: October 9, 2017
Accepted: October 10, 2017
Published: November 14, 2017

REFERENCES

Abe, M., and Bonini, N.M. (2013). MicroRNAs and neurodegeneration: role and impact. Trends Cell Biol. *23*, 30–36.

Aladjem, M.I., Spike, B.T., Rodewald, L.W., and Hope, T.J. (1998). ES cells do not activate p53-dependent stress responses and undergo p53-independent apoptosis in response to DNA damage. Curr. Biol. *8*, 145–155.

An, P., Saenz Robles, M.T., and Pipas, J.M. (2012). Large T antigens of polyomaviruses: amazing molecular machines. Annu. Rev. Microbiol. *66*, 213–236.

Anders, S., Pyl, P.T., and Huber, W. (2015). HTSeq–a Python framework to work with high-throughput sequencing data. Bioinformatics *31*, 166–169.

Andl, T., Murchison, E.P., Liu, F., Zhang, Y., Yunta-Gonzalez, M., Tobias, J.W., Andl, C.D., Seykora, J.T., Hannon, G.J., and Millar, S.E. (2006). The miRNA-processing enzyme dicer is essential for the morphogenesis and maintenance of hair follicles. Curr. Biol. *16*, 1041–1049.

Benetti, R., Gonzalo, S., Jaco, I., Munoz, P., Gonzalez, S., Schoeftner, S., Murchison, E., Andl, T., Chen, T., Klatt, P., et al. (2008). A mammalian microRNA cluster controls DNA methylation and telomere recombination via Rbl2-dependent regulation of DNA methyltransferases. Nat. Struct. Mol. Biol. *15*, 268–279.

Bernstein, E., Kim, S.Y., Carmell, M.A., Murchison, E.P., Alcorn, H., Li, M.Z., Mills, A.A., Elledge, S.J., Anderson, K.V., and Hannon, G.J. (2003). Dicer is essential for mouse development. Nat. Genet. *35*, 215–217.

Bolstad, B.M., Irizarry, R.A., Astrand, M., and Speed, T.P. (2003). A comparison of normalization methods for high density oligonucleotide array data based on variance and bias. Bioinformatics *19*, 185–193.

Card, D.A., Hebbar, P.B., Li, L., Trotter, K.W., Komatsu, Y., Mishina, Y., and Archer, T.K. (2008). Oct4/Sox2-regulated miR-302 targets cyclin D1 in human embryonic stem cells. Mol. Cell. Biol. *28*, 6426–6438.

Chambers, S.M., Fasano, C.A., Papapetrou, E.P., Tomishima, M., Sadelain, M., and Studer, L. (2009). Highly efficient neural conversion of human ES and iPS cells by dual inhibition of SMAD signaling. Nat. Biotechnol. *27*, 275–280.

Chapnik, E., Sasson, V., Blelloch, R., and Hornstein, E. (2012). Dgcr8 controls neural crest cells survival in cardiovascular development. Dev. Biol. *362*, 50–56.

Choi, P.S., Zakhary, L., Choi, W.Y., Caron, S., Alvarez-Saavedra, E., Miska, E.A., McManus, M., Harfe, B., Giraldez, A.J., Horvitz, H.R., et al. (2008). Members of the miRNA-200 family regulate olfactory neurogenesis. Neuron *57*, 41–55.

Cobb, B.S., Nesterova, T.B., Thompson, E., Hertweck, A., O'Connor, E., Godwin, J., Wilson, C.B., Brockdorff, N., Fisher, A.G., Smale, S.T., et al. (2005). T cell lineage choice and differentiation in the absence of the RNase III enzyme Dicer. J. Exp. Med. *201*, 1367–1373.

Davis, T.H., Cuellar, T.L., Koch, S.M., Barker, A.J., Harfe, B.D., McManus, M.T., and Ullian, E.M. (2008). Conditional loss of Dicer disrupts cellular and tissue morphogenesis in the cortex and hippocampus. J. Neurosci. *28*, 4322–4330.

De Pietri Tonelli, D., Pulvers, J.N., Haffner, C., Murchison, E.P., Hannon, G.J., and Huttner, W.B. (2008). miRNAs are essential for survival and differentiation of newborn neurons but not for expansion of neural progenitors during early neurogenesis in the mouse embryonic neocortex. Development *135*, 3911–3921.

Dobin, A., Davis, C.A., Schlesinger, F., Drenkow, J., Zaleski, C., Jha, S., Batut, P., Chaisson, M., and Gingeras, T.R. (2013). STAR: ultrafast universal RNA-seq aligner. Bioinformatics *29*, 15–21.

Donehower, L.A., Harvey, M., Slagle, B.L., McArthur, M.J., Montgomery, C.A., Jr., Butel, J.S., and Bradley, A. (1992). Mice deficient for p53 are developmentally normal but susceptible to spontaneous tumours. Nature *356*, 215–221.

Ewen, M.E., Ludlow, J.W., Marsilio, E., DeCaprio, J.A., Millikan, R.C., Cheng, S.H., Paucha, E., and Livingston, D.M. (1989). An N-Terminal transformation-governing sequence of SV40 large T antigen contributes to the binding of both p110Rb and a second cellular protein, p120. Cell *58*, 257–267.

Frum, T., Halbisen, M.A., Wang, C., Amiri, H., Robson, P., and Ralston, A. (2013). Oct4 cell-autonomously promotes primitive endoderm development in the mouse blastocyst. Dev. Cell *25*, 610–622.

Gentleman, R.C., Carey, V.J., Bates, D.M., Bolstad, B., Dettling, M., Dudoit, S., Ellis, B., Gautier, L., Ge, Y., Gentry, J., et al. (2004). Bioconductor: open software development for computational biology and bioinformatics. Genome Biol. *5*, R80.

Goomer, R.S., and Kunkel, G.R. (1992). The transcriptional start site for a human U6 small nuclear RNA gene is dictated by a compound promoter element consisting of the PSE and the TATA box. Nucleic Acids Res. *20*, 4903–4912.

Graham, V., Khudyakov, J., Ellis, P., and Pevny, L. (2003). SOX2 functions to maintain neural progenitor identity. Neuron *39*, 749–765.

Gu, S., Jin, L., Zhang, Y., Huang, Y., Zhang, F., Valdmanis, P.N., and Kay, M.A. (2012). The loop position of shRNAs and pre-miRNAs is critical for the accuracy of dicer processing in vivo. Cell *151*, 900–911.

Ha, M., and Kim, V.N. (2014). Regulation of microRNA biogenesis. Nat. Rev. Mol. Cell Biol. *15*, 509–524.

Harfe, B.D., McManus, M.T., Mansfield, J.H., Hornstein, E., and Tabin, C.J. (2005). The RNaseIII enzyme Dicer is required for morphogenesis but not patterning of the vertebrate limb. Proc. Natl. Acad. Sci. USA *102*, 10898–10903.

Hong, Y., and Stambrook, P.J. (2004). Restoration of an absent G1 arrest and protection from apoptosis in embryonic stem cells after ionizing radiation. Proc. Natl. Acad. Sci. USA *101*, 14443–14448.

Horn, H.F., and Vousden, K.H. (2007). Coping with stress: multiple ways to activate p53. Oncogene *26*, 1306–1316.

Hu, H.Y., Yan, Z., Xu, Y., Hu, H., Menzel, C., Zhou, Y.H., Chen, W., and Khaitovich, P. (2009). Sequence features associated with microRNA strand selection in humans and flies. BMC Genomics *10*, 413.

Hu, W., Feng, Z., Atwal, G.S., and Levine, A.J. (2008). p53: a new player in reproduction. Cell Cycle *7*, 848–852.

Irizarry, R.A., Hobbs, B., Collin, F., Beazer-Barclay, Y.D., Antonellis, K.J., Scherf, U., and Speed, T.P. (2003). Exploration, normalization, and summaries of high density oligonucleotide array probe level data. Biostatistics *4*, 249–264.

Ivey, K.N., and Srivastava, D. (2010). MicroRNAs as regulators of differentiation and cell fate decisions. Cell Stem Cell *7*, 36–41.

Kanellopoulou, C., Muljo, S.A., Kung, A.L., Ganesan, S., Drapkin, R., Jenuwein, T., Livingston, D.M., and Rajewsky, K. (2005). Dicer-deficient mouse embryonic stem cells are defective in differentiation and centromeric silencing. Genes Dev. *19*, 489–501.

Kastenhuber, E.R., and Lowe, S.W. (2017). Putting p53 in context. Cell *170*, 1062–1078.

Kawahara, H., Imai, T., and Okano, H. (2012). MicroRNAs in neural stem cells and neurogenesis. Front. Neurosci. *6*, 30.

Kawase-Koga, Y., Otaegi, G., and Sun, T. (2009). Different timings of Dicer deletion affect neurogenesis and gliogenesis in the developing mouse central nervous system. Dev. Dyn. *238*, 2800–2812.

Khoo, K.H., Verma, C.S., and Lane, D.P. (2014). Drugging the p53 pathway: understanding the route to clinical efficacy. Nat. Rev. Drug Discov. *13*, 217–236.

Kim, J., Inoue, K., Ishii, J., Vanti, W.B., Voronov, S.V., Murchison, E., Hannon, G., and Abeliovich, A. (2007). A microRNA feedback circuit in midbrain dopamine neurons. Science *317*, 1220–1224.

Kruse, J.P., and Gu, W. (2009). Modes of p53 regulation. Cell *137*, 609–622.

Kunkel, G.R., Maser, R.L., Calvet, J.P., and Pederson, T. (1986). U6 small nuclear RNA is transcribed by RNA polymerase III. Proc. Natl. Acad. Sci. USA *83*, 8575–8579.

Lane, D.P. (1992). Cancer. p53, guardian of the genome. Nature *358*, 15–16.

Lee, Y.S., and Dutta, A. (2009). MicroRNAs in cancer. Annu. Rev. Pathol. *4*, 199–227.

Leonardo, T.R., Schultheisz, H.L., Loring, J.F., and Laurent, L.C. (2012). The functions of microRNAs in pluripotency and reprogramming. Nat. Cell Biol. *14*, 1114–1121.

Levine, A.J. (1997). p53, the cellular gatekeeper for growth and division. Cell *88*, 323–331.

Li, M., He, Y., Dubois, W., Wu, X., Shi, J., and Huang, J. (2012). Distinct regulatory mechanisms and functions for p53-activated

and p53-repressed DNA damage response genes in embryonic stem cells. Mol. Cell *46*, 30–42.

Lin, T., Chao, C., Saito, S., Mazur, S.J., Murphy, M.E., Appella, E., and Xu, Y. (2005). p53 induces differentiation of mouse embryonic stem cells by suppressing Nanog expression. Nat. Cell Biol. *7*, 165–171.

Lipchina, I., Elkabetz, Y., Hafner, M., Sheridan, R., Mihailovic, A., Tuschl, T., Sander, C., Studer, L., and Betel, D. (2011). Genome-wide identification of microRNA targets in human ES cells reveals a role for miR-302 in modulating BMP response. Genes Dev. *25*, 2173–2186.

Liu, Z., Skamagki, M., Kim, K., and Zhao, R. (2015). Canonical microRNA activity facilitates but may be dispensable for transcription factor-mediated reprogramming. Stem Cell Reports *5*, 1119–1127.

Liu, Z., Zhang, C., Khodadadi-Jamayran, A., Dang, L., Han, X., Kim, K., Li, H., and Zhao, R. (2017). Canonical microRNAs enable differentiation, protect against DNA damage, and promote cholesterol biosynthesis in neural stem cells. Stem Cells Dev. *26*, 177–188.

Liu, Z., and Zhao, R. (2016). Generation of HEXA-deficient hiPSCs from fibroblasts of a Tay-Sachs disease patient. Stem Cell Res. *17*, 289–291.

Lu, W.J., Amatruda, J.F., and Abrams, J.M. (2009). p53 ancestry: gazing through an evolutionary lens. Nat. Rev. Cancer *9*, 758–762.

Makeyev, E.V., Zhang, J., Carrasco, M.A., and Maniatis, T. (2007). The MicroRNA miR-124 promotes neuronal differentiation by triggering brain-specific alternative pre-mRNA splicing. Mol. Cell *27*, 435–448.

Marino, S., Vooijs, M., van Der Gulden, H., Jonkers, J., and Berns, A. (2000). Induction of medulloblastomas in p53-null mutant mice by somatic inactivation of Rb in the external granular layer cells of the cerebellum. Genes Dev. *14*, 994–1004.

Melton, C., Judson, R.L., and Blelloch, R. (2010). Opposing microRNA families regulate self-renewal in mouse embryonic stem cells. Nature *463*, 621–626.

Messerschmidt, D.M., and Kemler, R. (2010). Nanog is required for primitive endoderm formation through a non-cell autonomous mechanism. Dev. Biol. *344*, 129–137.

Moffat, J., Grueneberg, D.A., Yang, X., Kim, S.Y., Kloepfer, A.M., Hinkle, G., Piqani, B., Eisenhaure, T.M., Luo, B., Grenier, J.K., et al. (2006). A lentiviral RNAi library for human and mouse genes applied to an arrayed viral high-content screen. Cell *124*, 1283–1298.

Murchison, E.P., Partridge, J.F., Tam, O.H., Cheloufi, S., and Hannon, G.J. (2005). Characterization of Dicer-deficient murine embryonic stem cells. Proc. Natl. Acad. Sci. USA *102*, 12135–12140.

Nie, X., Wang, Q., and Jiao, K. (2011). Dicer activity in neural crest cells is essential for craniofacial organogenesis and pharyngeal arch artery morphogenesis. Mech. Dev. *128*, 200–207.

Parchem, R.J., Moore, N., Fish, J.L., Parchem, J.G., Braga, T.T., Shenoy, A., Oldham, M.C., Rubenstein, J.L., Schneider, R.A., and Blelloch, R. (2015). miR-302 is required for timing of neural differentiation, neural tube closure, and embryonic viability. Cell Rep. *12*, 760–773.

Parchem, R.J., Ye, J., Judson, R.L., LaRussa, M.F., Krishnakumar, R., Blelloch, A., Oldham, M.C., and Blelloch, R. (2014). Two miRNA clusters reveal alternative paths in late-stage reprogramming. Cell Stem Cell *14*, 617–631.

Purvis, J.E., Karhohs, K.W., Mock, C., Batchelor, E., Loewer, A., and Lahav, G. (2012). p53 dynamics control cell fate. Science *336*, 1440–1444.

Qin, H., Yu, T., Qing, T., Liu, Y., Zhao, Y., Cai, J., Li, J., Song, Z., Qu, X., Zhou, P., et al. (2007). Regulation of apoptosis and differentiation by p53 in human embryonic stem cells. J. Biol. Chem. *282*, 5842–5852.

Roos, W.P., Christmann, M., Fraser, S.T., and Kaina, B. (2007). Mouse embryonic stem cells are hypersensitive to apoptosis triggered by the DNA damage O(6)-methylguanine due to high E2F1 regulated mismatch repair. Cell Death Differ. *14*, 1422–1432.

Sinkkonen, L., Hugenschmidt, T., Berninger, P., Gaidatzis, D., Mohn, F., Artus-Revel, C.G., Zavolan, M., Svoboda, P., and Filipowicz, W. (2008). MicroRNAs control de novo DNA methylation through regulation of transcriptional repressors in mouse embryonic stem cells. Nat. Struct. Mol. Biol. *15*, 259–267.

Spike, B.T., and Wahl, G.M. (2011). p53, stem cells, and reprogramming: tumor suppression beyond guarding the genome. Genes Cancer *2*, 404–419.

Storey, J.D., and Tibshirani, R. (2003). Statistical significance for genomewide studies. Proc. Natl. Acad. Sci. USA *100*, 9440–9445.

Subramanian, A., Tamayo, P., Mootha, V.K., Mukherjee, S., Ebert, B.L., Gillette, M.A., Paulovich, A., Pomeroy, S.L., Golub, T.R., Lander, E.S., et al. (2005). Gene set enrichment analysis: a knowledge-based approach for interpreting genome-wide expression profiles. Proc. Natl. Acad. Sci. USA *102*, 15545–15550.

Subramanyam, D., Lamouille, S., Judson, R.L., Liu, J.Y., Bucay, N., Derynck, R., and Blelloch, R. (2011). Multiple targets of miR-302 and miR-372 promote reprogramming of human fibroblasts to induced pluripotent stem cells. Nat. Biotechnol. *29*, 443–448.

Suh, M.R., Lee, Y., Kim, J.Y., Kim, S.K., Moon, S.H., Lee, J.Y., Cha, K.Y., Chung, H.M., Yoon, H.S., Moon, S.Y., et al. (2004). Human embryonic stem cells express a unique set of microRNAs. Dev. Biol. *270*, 488–498.

Tiscornia, G., and Izpisua Belmonte, J.C. (2010). MicroRNAs in embryonic stem cell function and fate. Genes Dev. *24*, 2732–2741.

Vassilev, L.T., Vu, B.T., Graves, B., Carvajal, D., Podlaski, F., Filipovic, Z., Kong, N., Kammlott, U., Lukacs, C., Klein, C., et al. (2004). In vivo activation of the p53 pathway by small-molecule antagonists of MDM2. Science *303*, 844–848.

Wang, Y., Baskerville, S., Shenoy, A., Babiarz, J.E., Baehner, L., and Blelloch, R. (2008). Embryonic stem cell-specific microRNAs regulate the G1-S transition and promote rapid proliferation. Nat. Genet. *40*, 1478–1483.

Wang, Y., Medvid, R., Melton, C., Jaenisch, R., and Blelloch, R. (2007). DGCR8 is essential for microRNA biogenesis and silencing of embryonic stem cell self-renewal. Nat. Genet. *39*, 380–385.

Wang, Y., Melton, C., Li, Y.P., Shenoy, A., Zhang, X.X., Subramanyam, D., and Blelloch, R. (2013). miR-294/miR-302 promotes proliferation, suppresses G1-S restriction point, and inhibits ESC differentiation through separable mechanisms. Cell Rep. *4*, 99–109.

Xu, N., Papagiannakopoulos, T., Pan, G., Thomson, J.A., and Kosik, K.S. (2009). MicroRNA-145 regulates OCT4, SOX2, and KLF4 and represses pluripotency in human embryonic stem cells. Cell *137*, 647–658.

Zhao, J.J., Gjoerup, O.V., Subramanian, R.R., Cheng, Y., Chen, W., Roberts, T.M., and Hahn, W.C. (2003). Human mammary epithelial cell transformation through the activation of phosphatidylinositol 3-kinase. Cancer Cell *3*, 483–495.

Zhao, R., Deibler, R.W., Lerou, P.H., Ballabeni, A., Heffner, G.C., Cahan, P., Unternaehrer, J.J., Kirschner, M.W., and Daley, G.Q. (2014). A nontranscriptional role for Oct4 in the regulation of mitotic entry. Proc. Natl. Acad. Sci. USA *111*, 15768–15773.